

Electronic Supplementary Information

Relative stability and reducibility of CeO₂ and Rh/CeO₂ species on the surface and in the cavities of γ -Al₂O₃: A periodic DFT study

Iskra Z. Koleva,^a Hristiyan A. Aleksandrov,^a Georgi N. Vayssilov,^{a,*} Renata Duarte,^b Jeroen A. van Bokhoven^{b,c,*}

^a Faculty of Chemistry and Pharmacy, University of Sofia, 1126 Sofia, Bulgaria
e-mail: gnv@chem.uni-sofia.bg

^b Institute for Chemical and Bioengineering, ETH Zurich, Zurich, Switzerland

^c Laboratory for Catalysis and Sustainable Chemistry, Swiss Light Source, Paul Scherrer Institute, Villigen, Switzerland, j.a.vanbokhoven@chem.ethz.ch

Content:

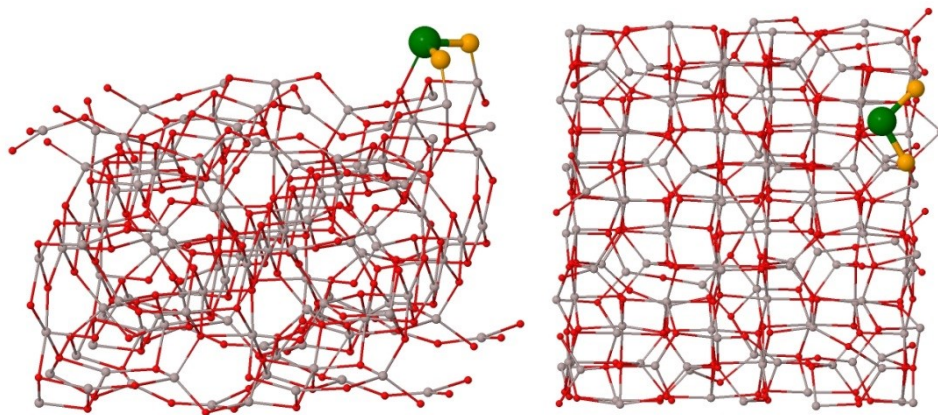
1. Table S1: Average displacement of Al and O ions of (100) and (001) γ -Al₂O₃ slabs
2. Figure S1: Optimized structures of stoichiometric one ceria unit on γ -Al₂O₃(100).
3. Figure S2: Optimized structures of two ceria units and one Ce₂O₃ deposited or inside cavities of γ -Al₂O₃(100).
4. Figure S3: Optimized structures of deposited ceria nanoparticle and incorporated in the bulk of γ -Al₂O₃(100) ceria species.
5. Figure S4: Optimized structures of deposited/incorporated stoichiometric or reduced ceria units on γ -Al₂O₃(001).
6. Figure S5: Optimized structures of deposited ceria nanoparticle and incorporated in the bulk of γ -Al₂O₃(001) ceria species.
7. Figure S6: Representation of Al and O ions from the slab with large displacement - equal to or above 1.2 Å (colored in black and yellow, respectively) in some structures with deposited or incorporated stoichiometric ceria species.
8. Description of the approach for simulation of the relative concentrations of reduced and stoichiometric ceria nanoparticles on γ -Al₂O₃(100) surface using enthalpy and entropy values obtained from computational results.
9. Discussion on interatomic distances in the different structures.

Color coding for all figures: Ce⁴⁺ - green, Ce³⁺ - cyan, O from CeO₂ species - orange, Al - gray, O - red, exchanged Al - dark blue.

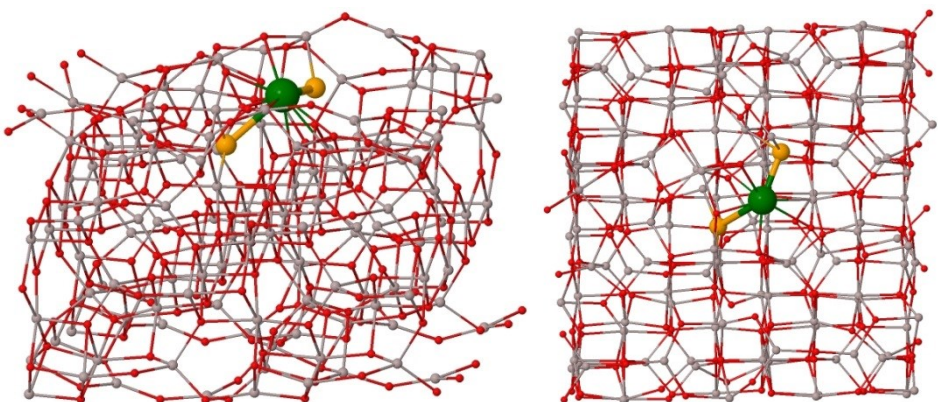
Table S1. Comparison between the average displacement of all Al and O ions of γ -Al₂O₃ and only for surface Al and O (in Å) in different structures with deposited or incorporated stoichiometric ceria species.

Structure	Description	Al	O	Surface Al	Surface O
γ-Al₂O₃(100)					
A-1a	CeO ₂ deposited	0.317	0.318	0.487	0.389
A-1b	CeO ₂ in subsurface cavity	0.398	0.374	0.664	0.618
A-1c	CeO ₂ in internal cavity	0.461	0.448	0.840	0.869
A-2a	2CeO ₂ deposited	0.314	0.321	0.516	0.541
A-2c	2CeO ₂ in identical subsurface cavities	0.512	0.514	0.937	1.034
A-2e	2CeO ₂ internal cavities	0.568	0.590	0.792	0.891
A-13a	Ce ₁₃ O ₂₆ deposited	0.102	0.083	0.235	0.178
A-13b	Ce ₁₂ O ₂₄ deposited, 1CeO ₂ subsurface	0.312	0.290	0.617	0.529
A-13c	Ce ₁₁ O ₂₂ deposited, 2CeO ₂ subsurface	0.394	0.378	0.783	0.728
γ-Al₂O₃(001)					
B-1a	CeO ₂ deposited	0.023	0.021	0.004	0.006
B-1b	CeO ₂ subsurface cavity	0.122	0.098	0.473	0.393
B-1c	CeO ₂ internal cavity	0.139	0.132	0.132	0.140
B-2a	2CeO ₂ deposited	0.040	0.033	0.010	0.011
B-2b	2CeO ₂ in identical subsurface	0.212	0.205	0.720	0.664
B-4a	4CeO ₂ deposited	0.045	0.038	0.014	0.017
B-4b	3CeO ₂ deposited, 1CeO ₂ subsurface	0.108	0.139	0.053	0.053
B-13a	Ce ₁₃ O ₂₆ deposited	0.051	0.045	0.028	0.034
B-13b	Ce ₁₂ O ₂₄ deposited, 1CeO ₂ subsurface	0.173	0.146	0.059	0.058

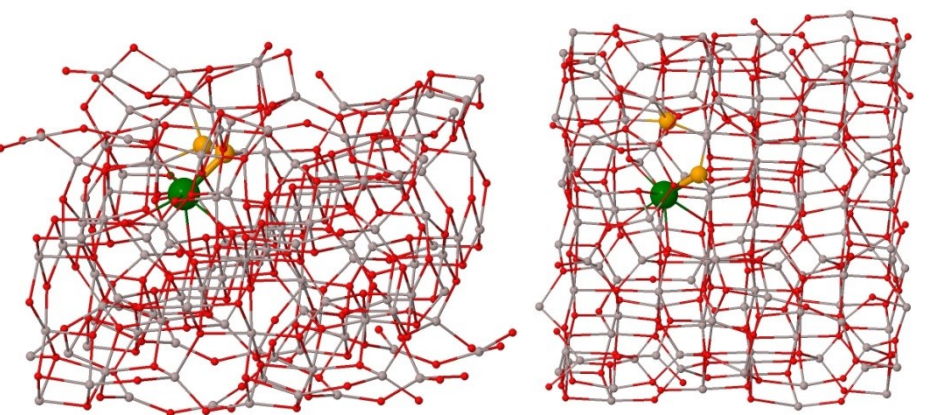
A-1a



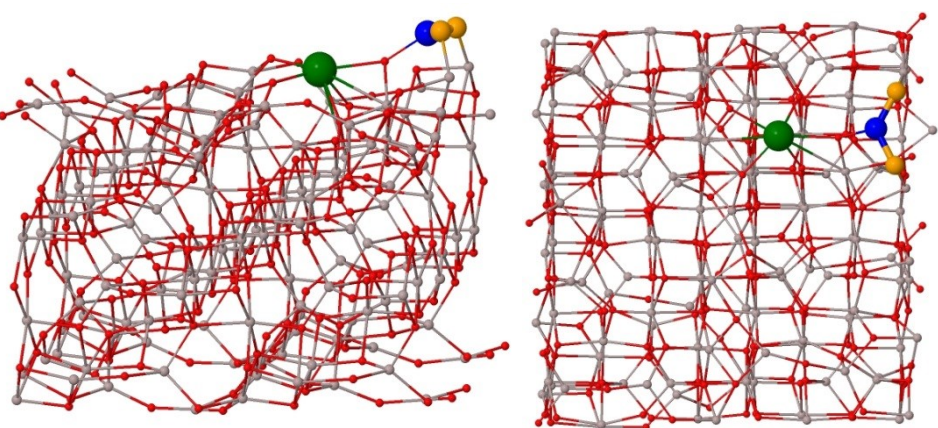
A-1b



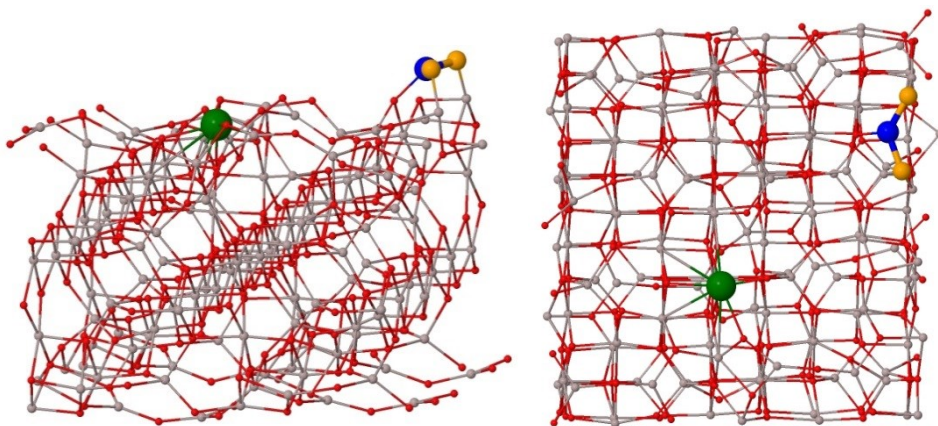
A-1c



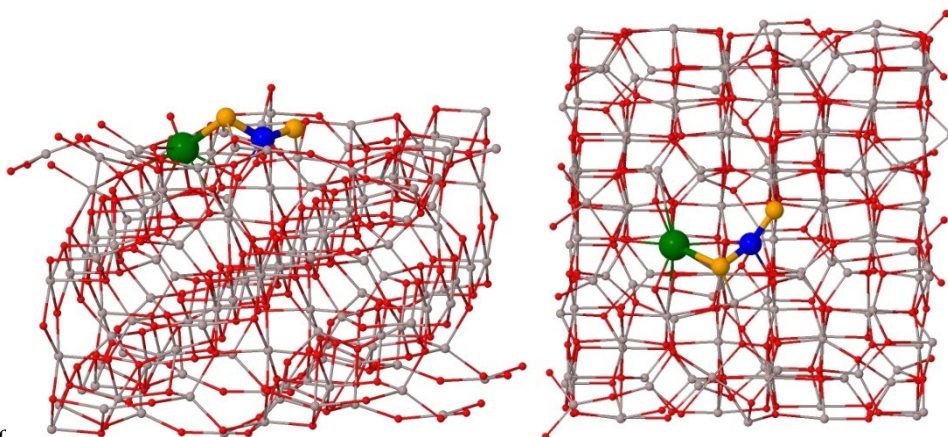
A-1d



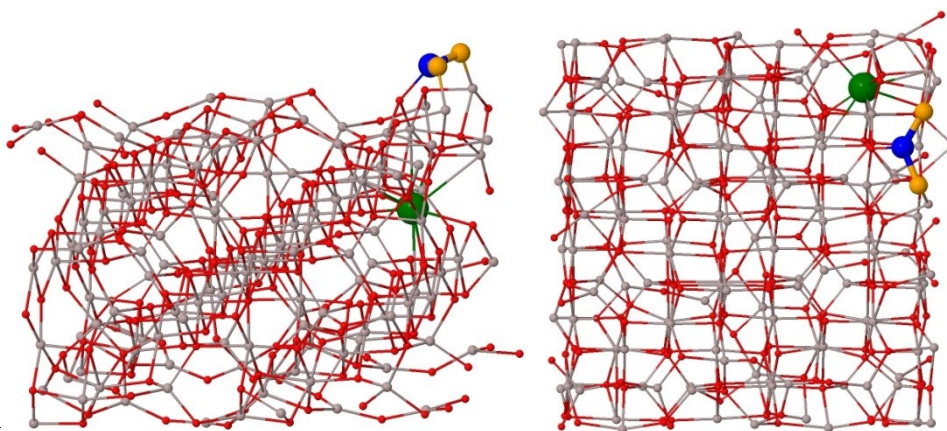
A-1e



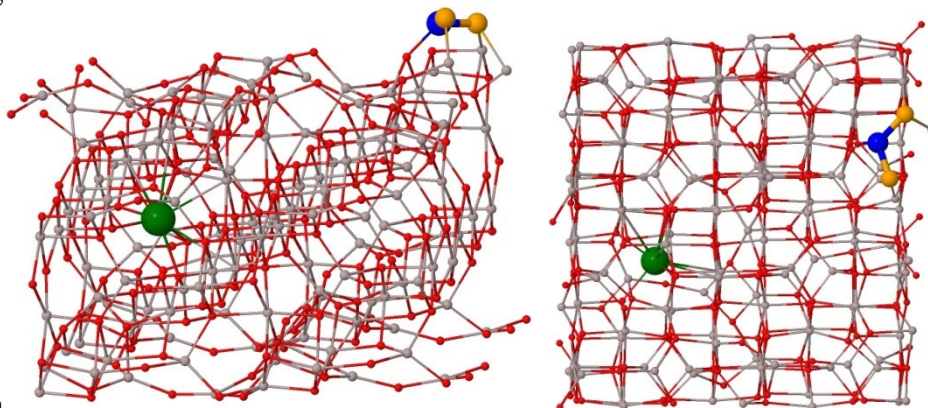
A-1f

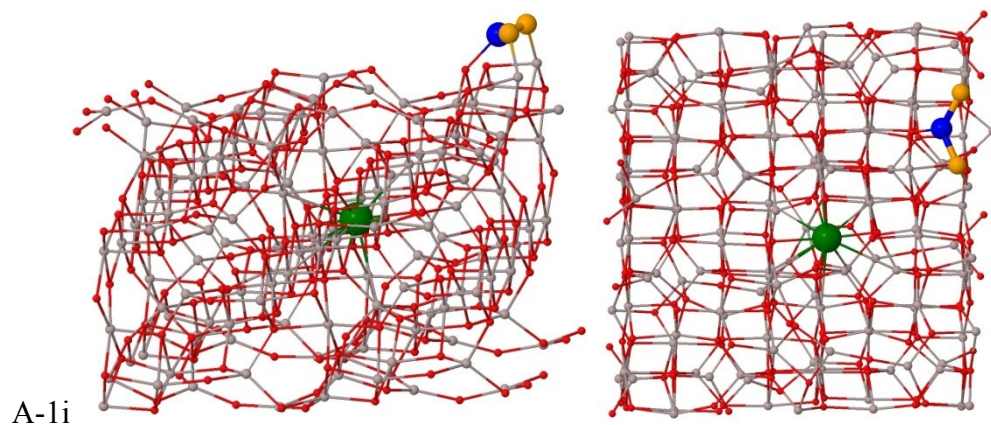


A-1g



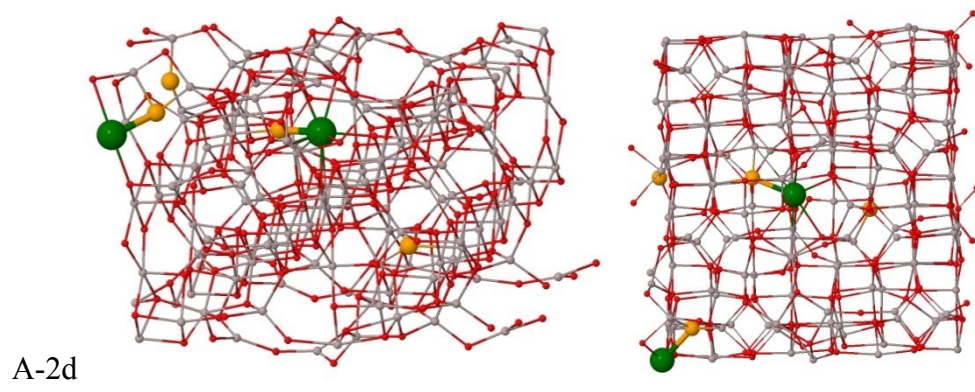
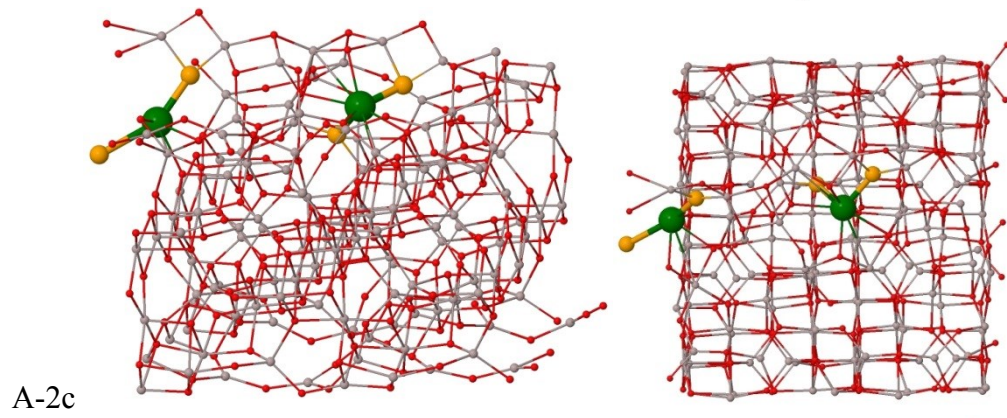
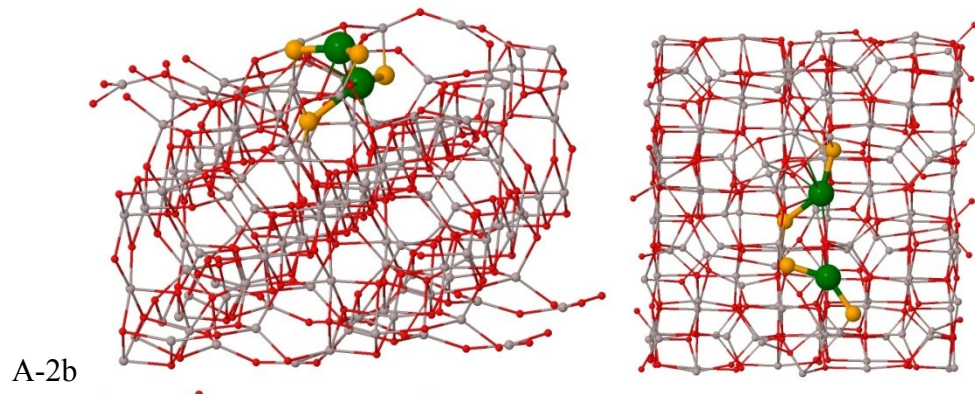
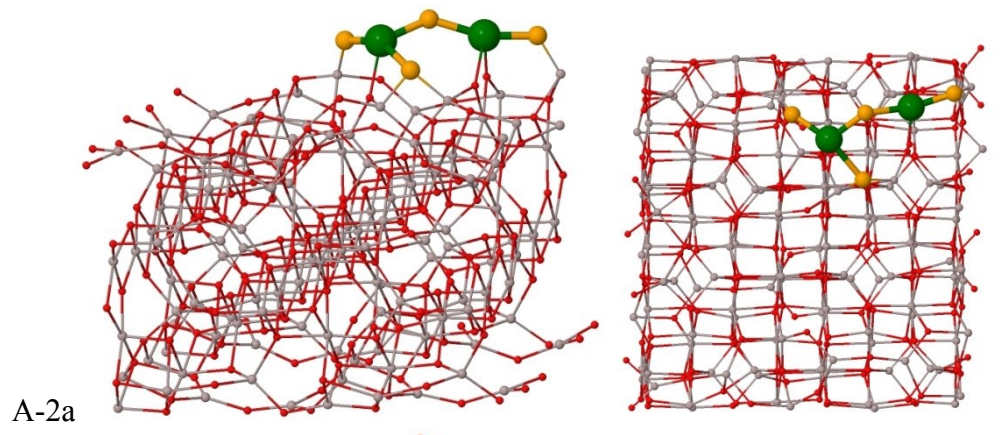
A-1h

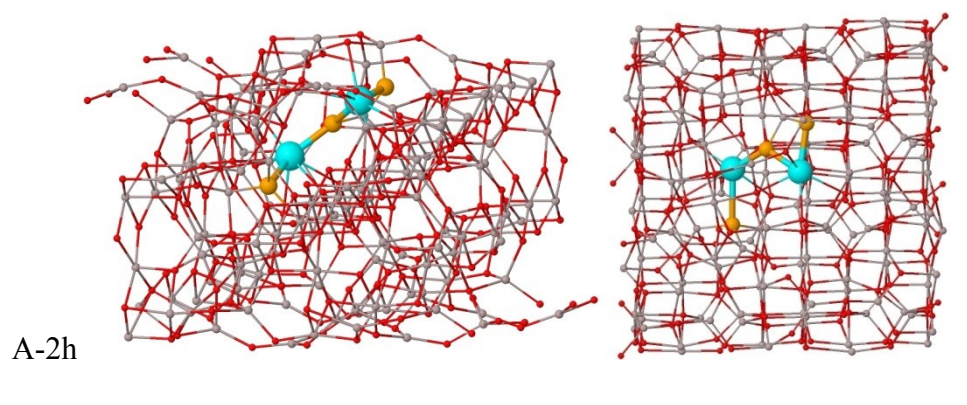
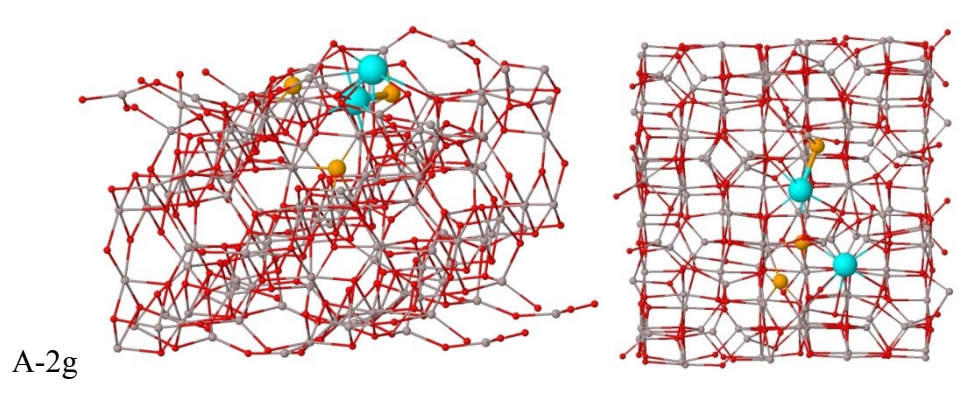
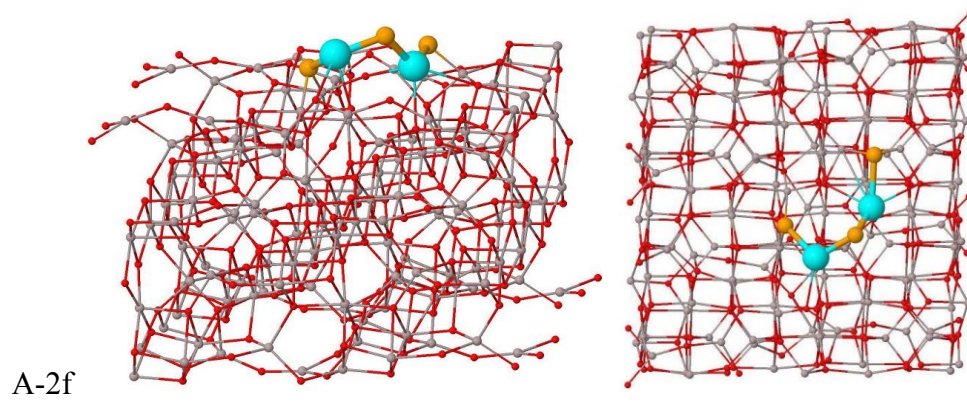
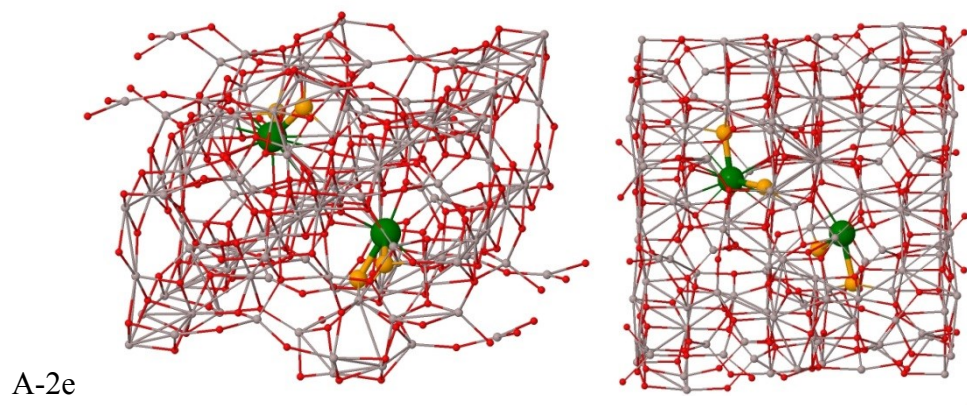




A-1i

Figure S1. Optimized models of stoichiometric one ceria unit on $\gamma\text{-Al}_2\text{O}_3(100)$: A-1a - one deposited unit; A-1b - one unit CeO_2 in subsurface cavity A-1c - one unit CeO_2 in internal cavity; A-1d-exchanged surface Al(3O); A-1e and A-1f - exchanged surface Al(5O); A-1g and A-1h - exchanged bulk Al(4O); A-1i – exchanged bulk Al(6O).





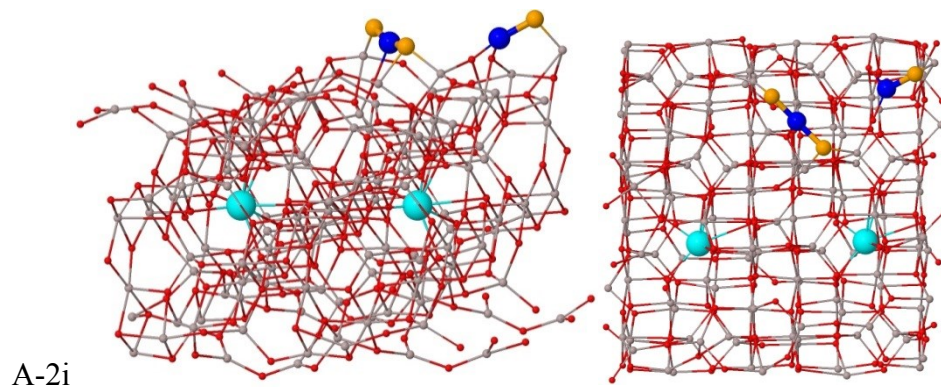
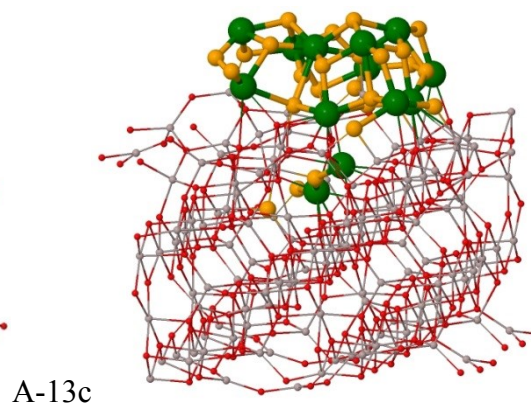
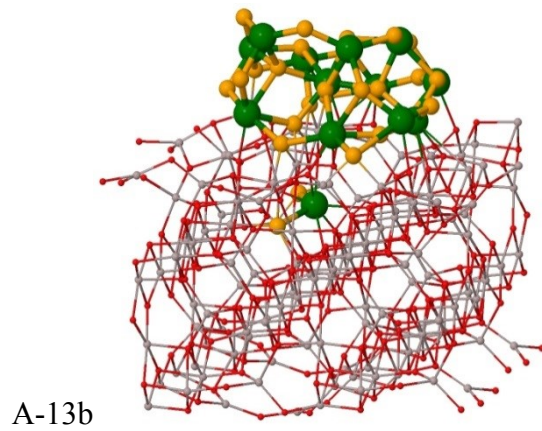
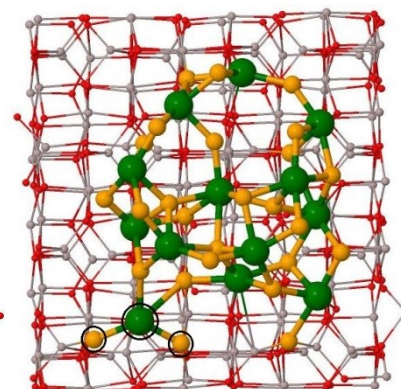
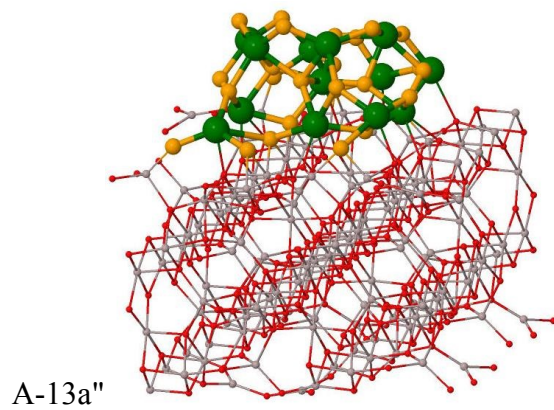
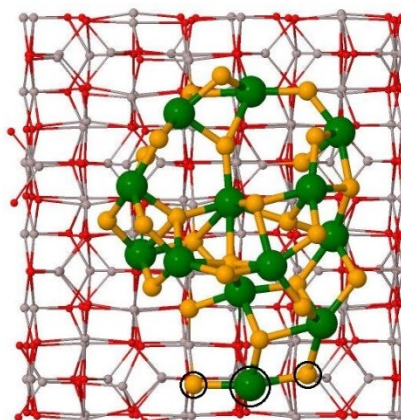
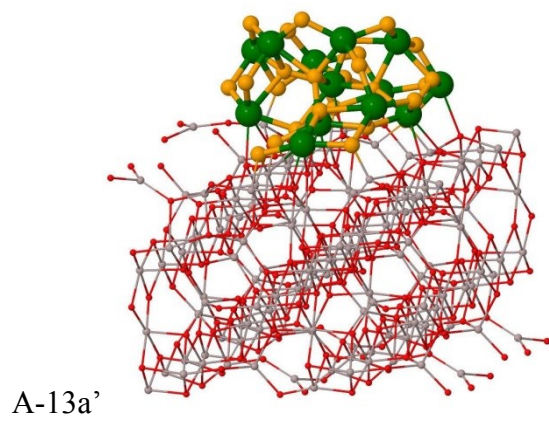
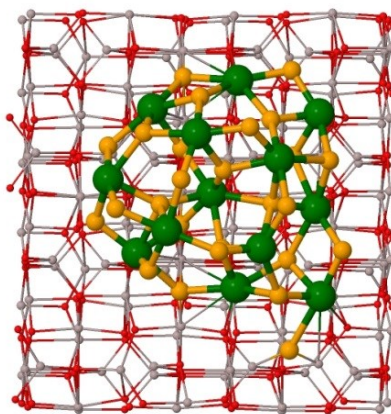
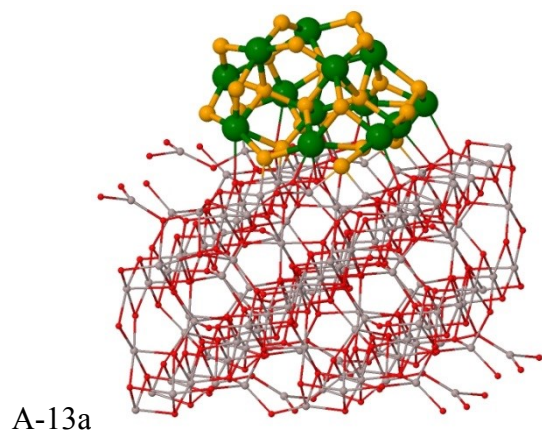
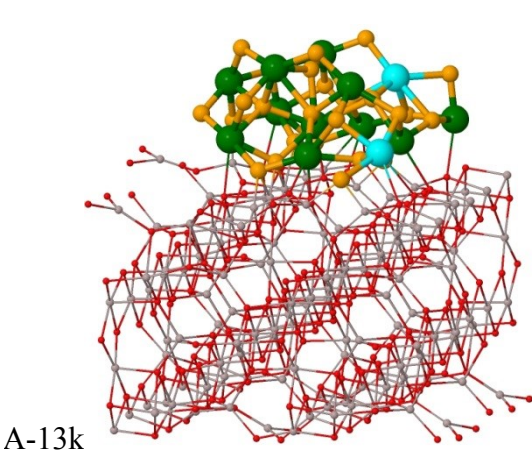
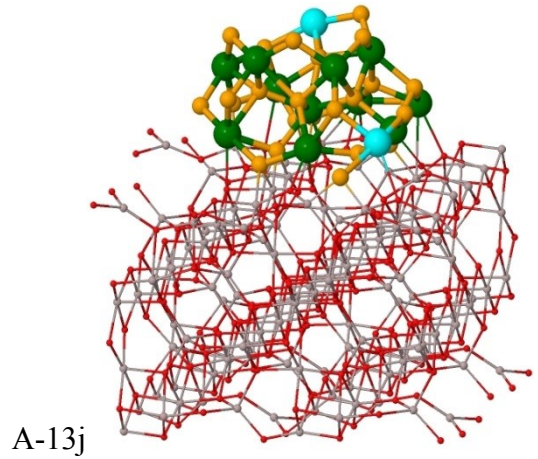
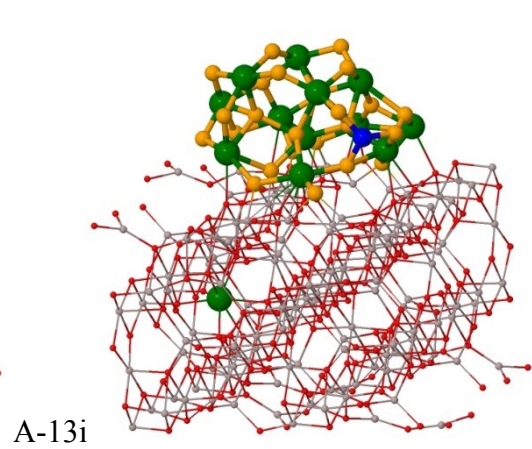
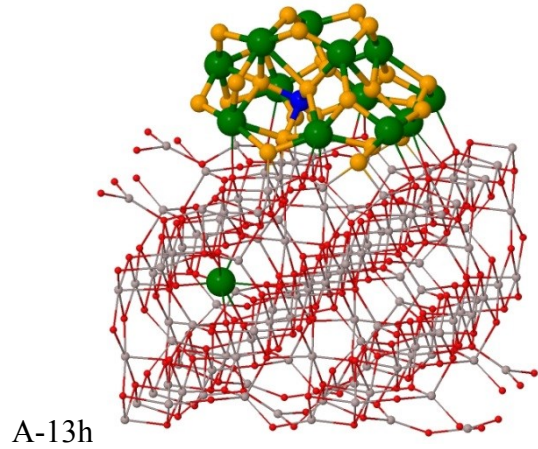
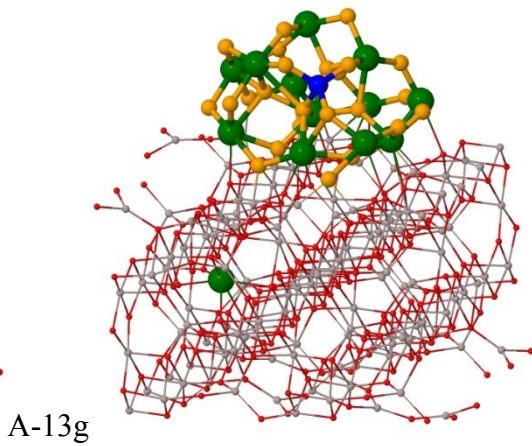
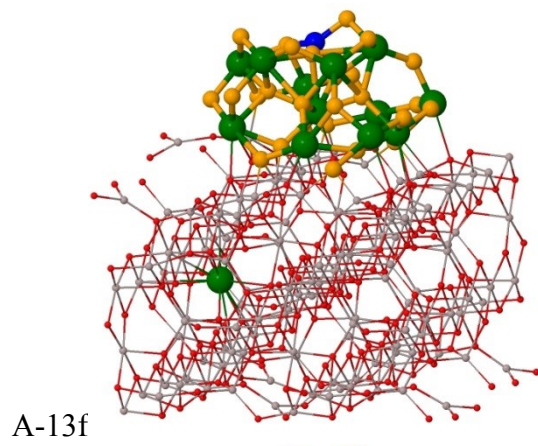
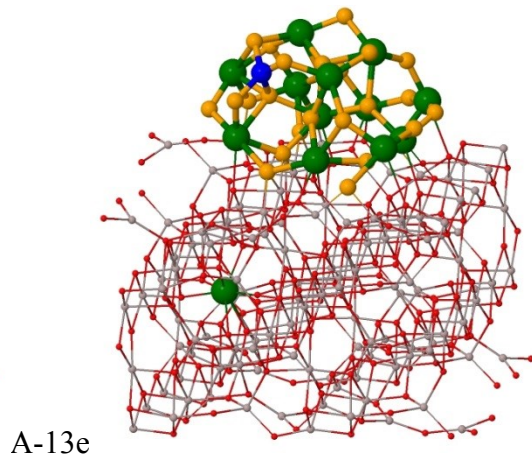
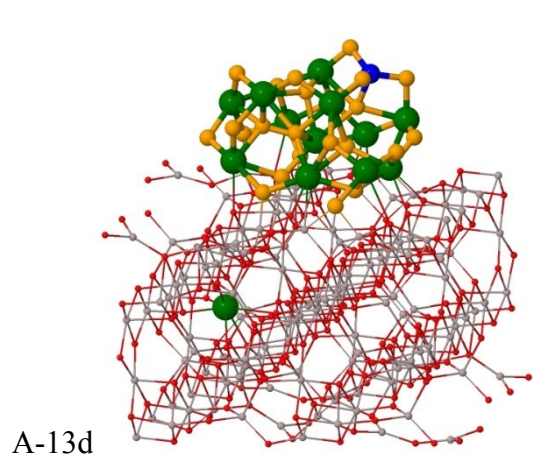


Figure S2. Optimized models of two Ce^{4+} or Ce^{3+} cations on $\gamma\text{-Al}_2\text{O}_3(100)$: A-2a-two deposited ceria units; A-2b - one deposited unit and one in subsurface cavity; A-2c - two units in identical subsurface cavities; A-2d one unit on subsurface, one in internal cavity; A-2e - 2CeO_2 in internal cavities; A-2f -deposited Ce_2O_3 unit; A-2g-two Ce^{3+} cations in subsurface cavity; A-2h one Ce^{3+} in subsurface, one - in internal cavity; A-2i-exchange of 2Ce^{3+} with internal 2Al^{3+} .





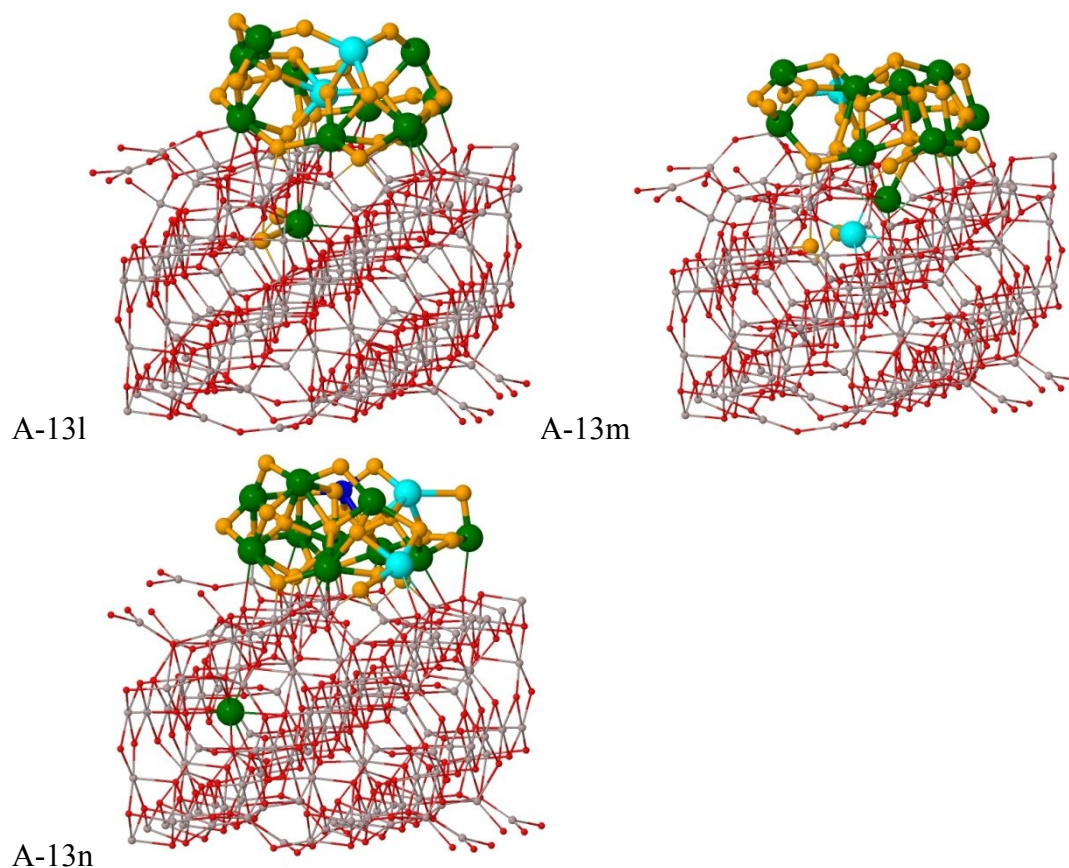
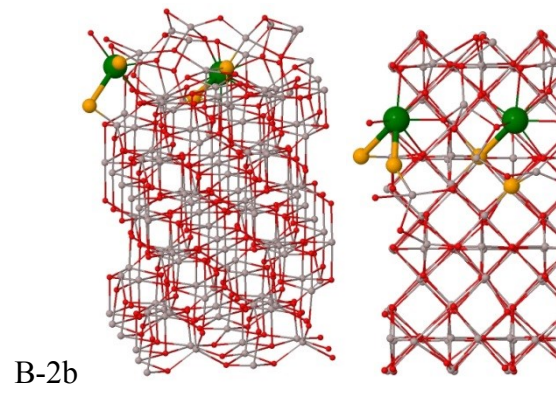
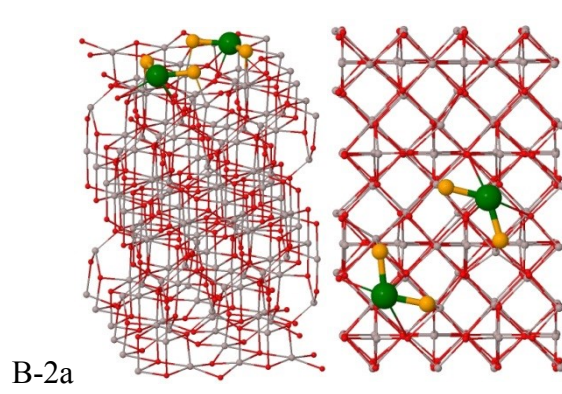
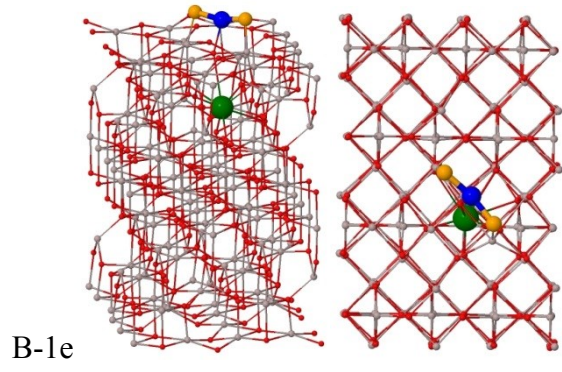
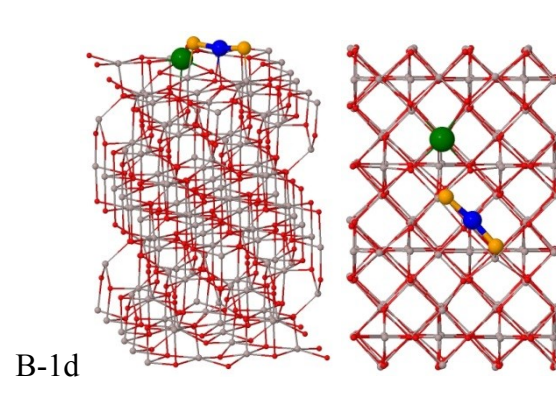
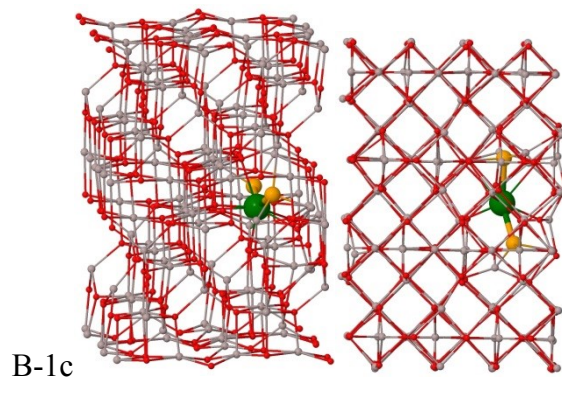
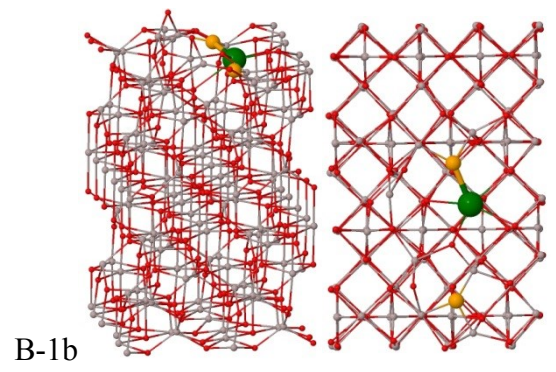
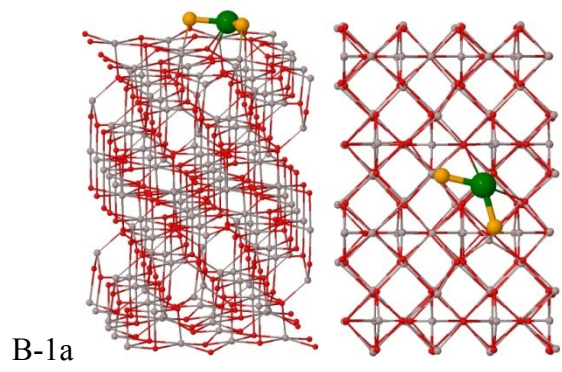


Figure S3. Optimized structures of stoichiometric or reduced ceria nanoparticle on γ - $\text{Al}_2\text{O}_3(100)$: A-13a - deposited $\text{Ce}_{13}\text{O}_{26}$ nanoparticle, A-13a' and A-13a'' - deposited $\text{Ce}_{12}\text{O}_{24}$ nanoparticle and one CeO_2 unit from the top layer deposited on the surface (the deposited CeO_2 unit is marked with black circles in the top view panels); A-13b - deposited $\text{Ce}_{12}\text{O}_{24}$ nanoparticle and one CeO_2 unit in subsurface cavity; A-13c - $\text{Ce}_{11}\text{O}_{22}$ deposited, two units CeO_2 in subsurface cavities; A-13d - one of the top Ce^{4+} cations is exchanged with Al^{3+} from the bulk; A-13e-g - exchange of one Ce^{4+} from the top layer of the nanoparticle with bulk Al^{3+} ; A-13h-i exchange of one Ce^{4+} cation from the top layer of the nanoparticle with bulk Al^{3+} ; A-13j-k - deposited reduced $\text{Ce}_{13}\text{O}_{25}$ nanoparticle; A-13l - $\text{Ce}_{12}\text{O}_{23}$ deposited and one CeO_2 unit in subsurface cavity; A-13m - $\text{Ce}_{12}\text{O}_{23}$ deposited, one Ce^{3+} cation and one CeO_2 unit in subsurface cavity; A-13n - deposited $\text{Ce}_{13}\text{O}_{25}$ with exchange of one Ce^{4+} cation with bulk Al^{3+} .



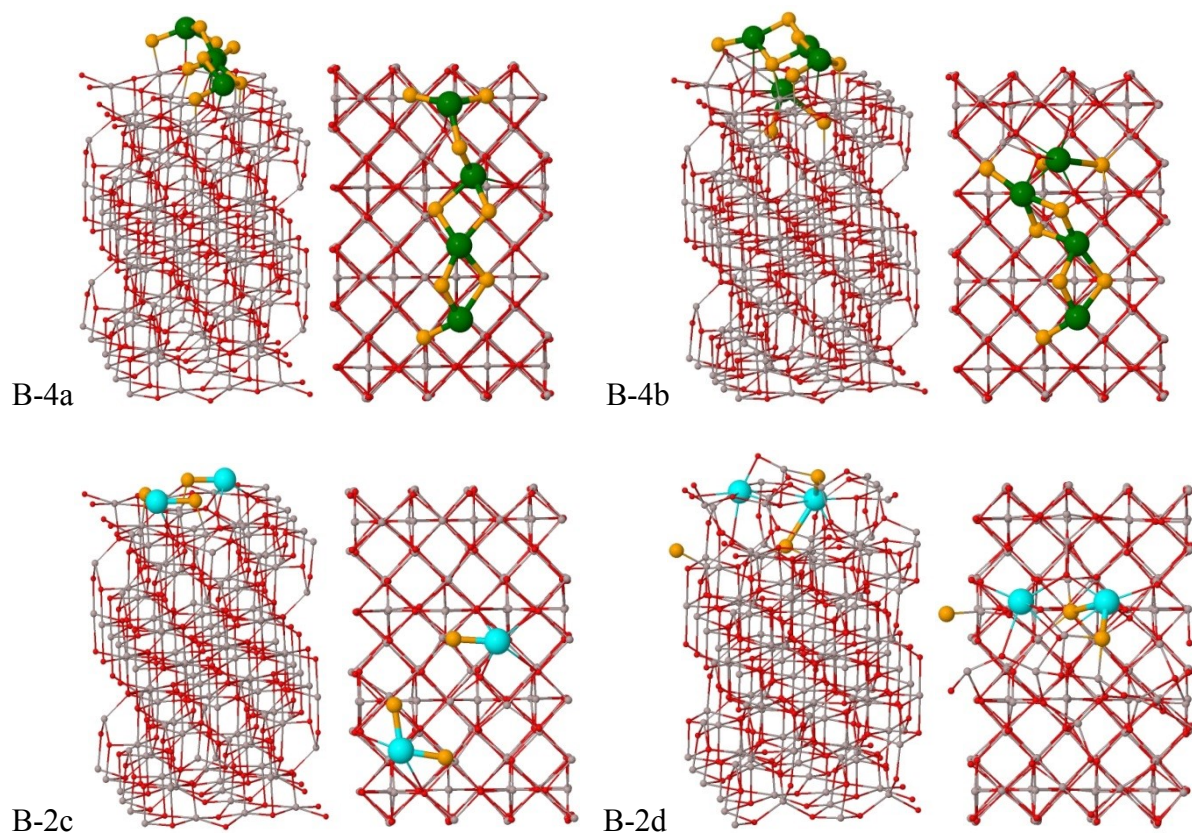


Figure S4. Optimized structures of stoichiometric or reduced CeO_2 species on $\gamma\text{-Al}_2\text{O}_3(001)$: B-1a - deposited CeO_2 unit; B-1b - CeO_2 unit in subsurface cavity; B-1c -one CeO_2 unit in internal cavity; B-1d - exchange of Ce^{4+} with surface $\text{Al}^{3+}(5\text{O})$; B-1e - exchange of Ce^{4+} with internal $\text{Al}^{3+}(4\text{O})$; B-2a - two deposited CeO_2 units; B-2b - two CeO_2 units in identical subsurface cavities; B-4a - four deposited CeO_2 units; B-4b - three deposited CeO_2 units and one in a subsurface cavity; B-2c - two deposited Ce^{3+} cations; B-2d - two Ce^{3+} cations in identical subsurface.

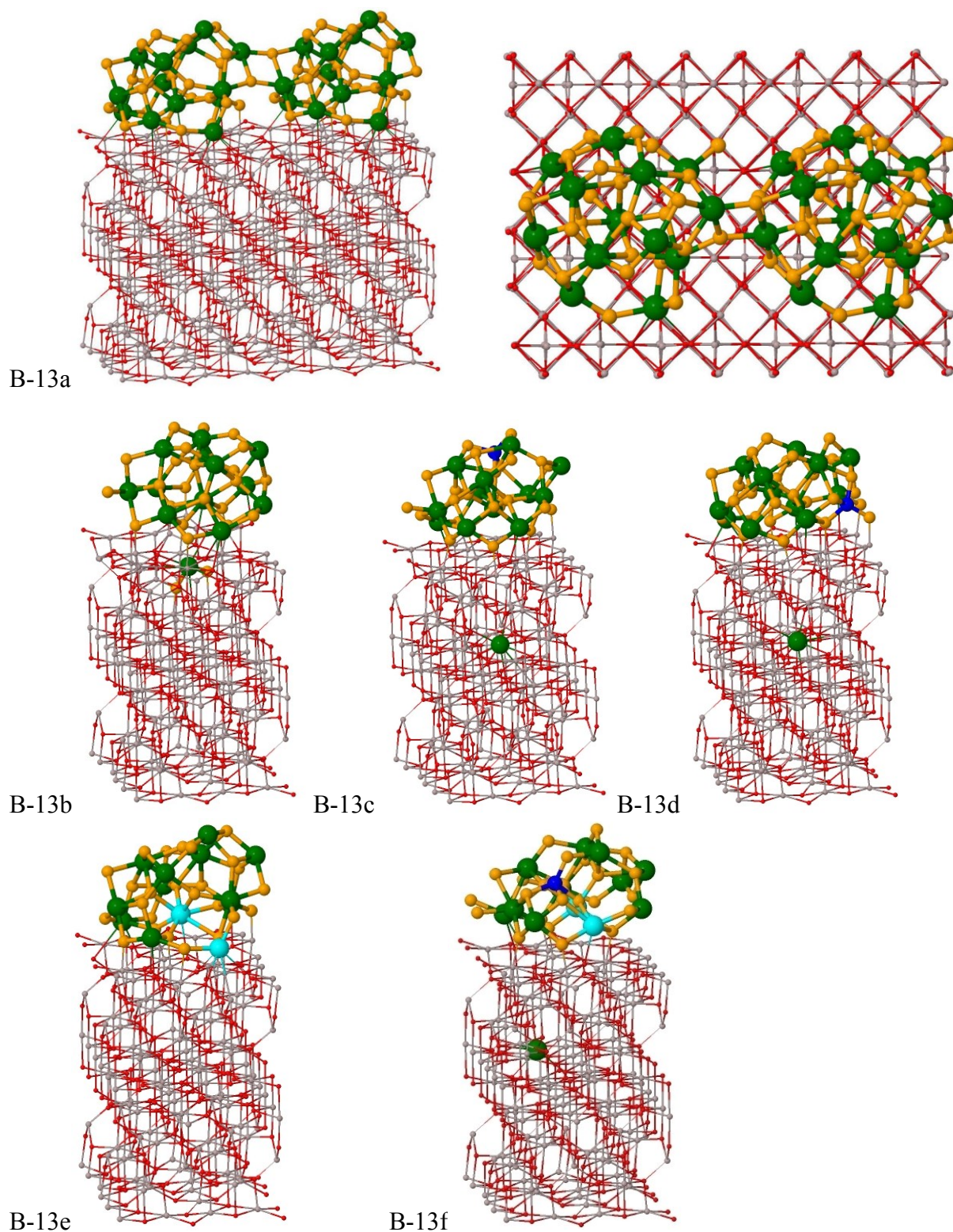
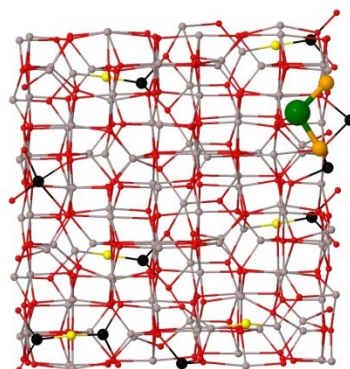
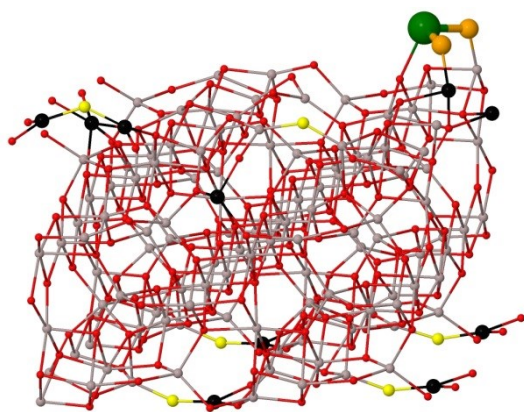
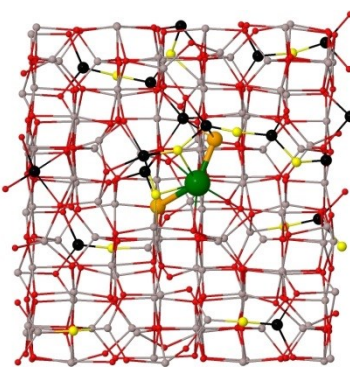
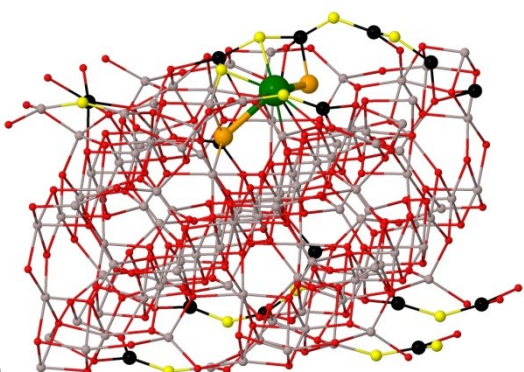


Figure S5. Optimized structures of stoichiometric or reduced ceria nanoparticle on γ - $\text{Al}_2\text{O}_3(001)$: B-13a - deposited $\text{Ce}_{13}\text{O}_{26}$ nanoparticle; B-13b - deposited $\text{Ce}_{12}\text{O}_{24}$ nanoparticle and one CeO_2 unit in subsurface cavity; B-13c - deposited $\text{Ce}_{13}\text{O}_{26}$ nanoparticle with exchange of top 1Ce^{4+} with internal Al^{3+} ; B-13d - deposited $\text{Ce}_{13}\text{O}_{26}$ with exchange of bottom Ce^{4+} cation with internal Al^{3+} ; B-13e - deposited $\text{Ce}_{13}\text{O}_{25}$ nanoparticle; B-13f - exchange of bulk Al^{3+} with Ce^{4+} cation from the top layer of the reduced nanoparticle.

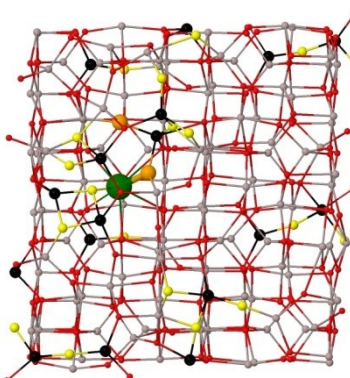
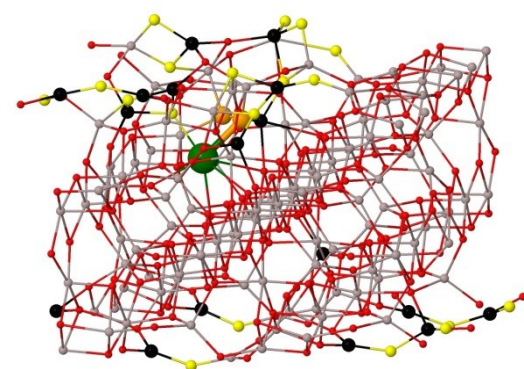
A-1a



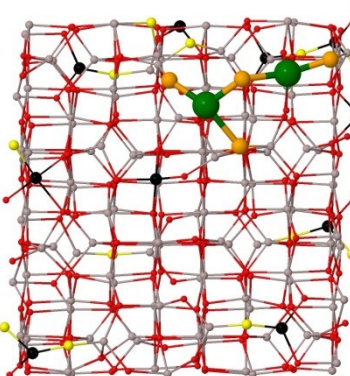
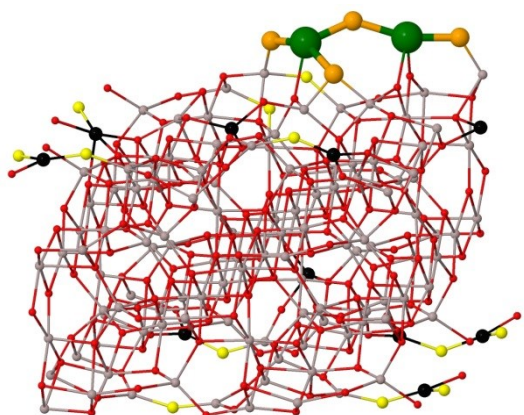
A-1b

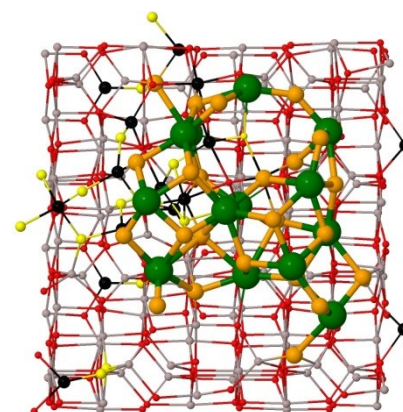
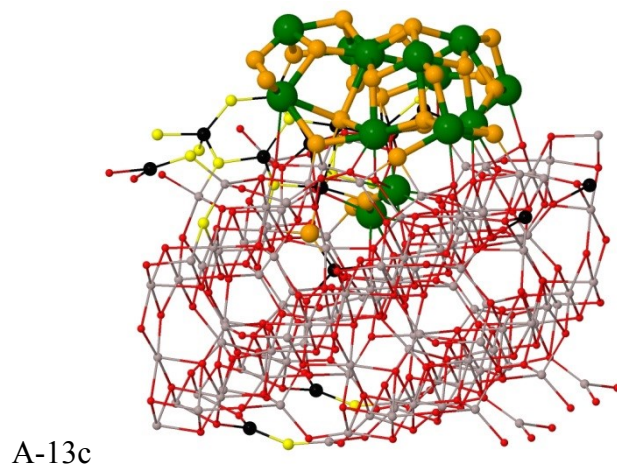
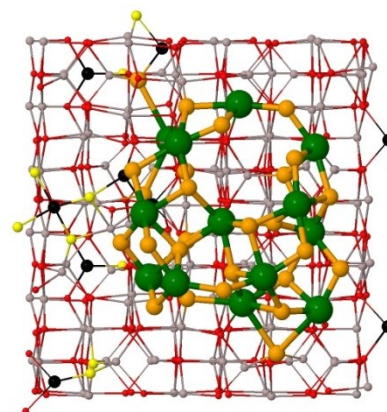
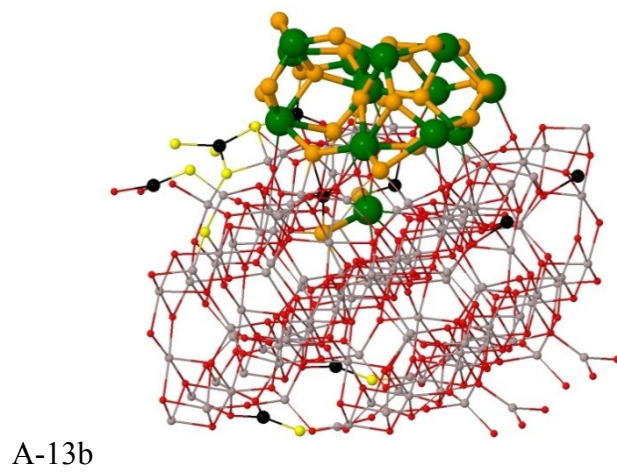
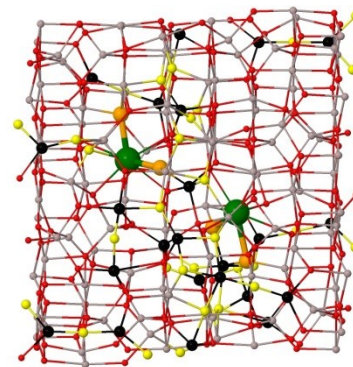
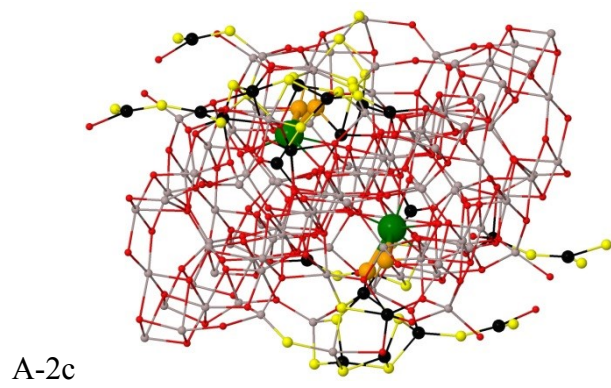
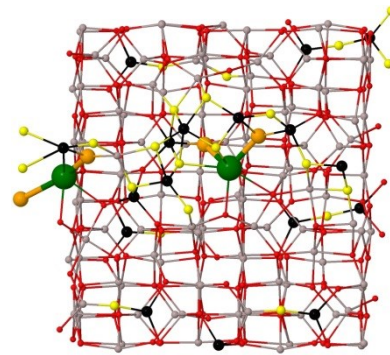
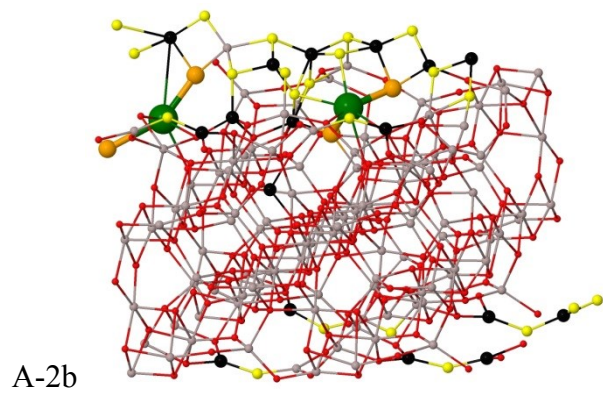


A-1c



A-2a





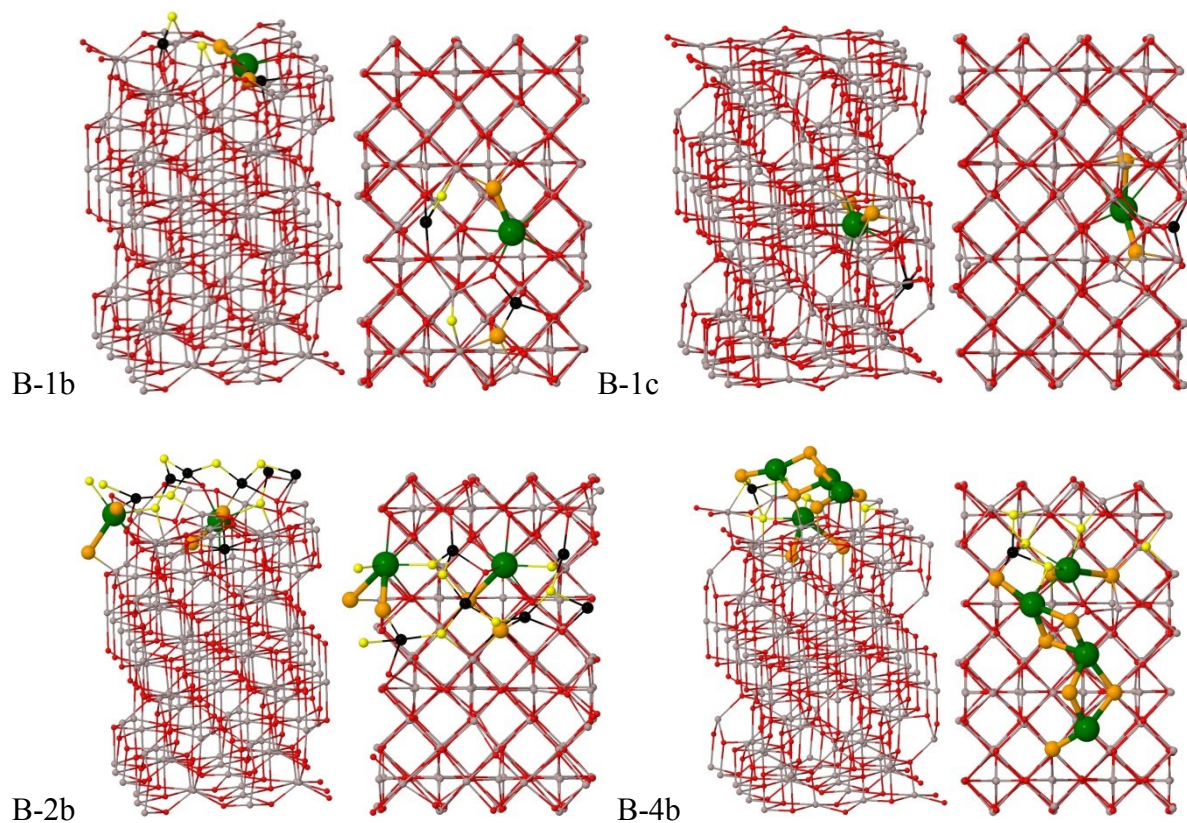


Figure S6. Representation of Al and O ions from the slab with large displacement - equal to or above 1.2 Å (colored in black and yellow, respectively) in some structures with deposited or incorporated stoichiometric ceria species : A-1a - one deposited unit; A-1b - one unit CeO_2 in subsurface cavity A-1c - one unit CeO_2 in internal cavity; A-2a-two deposited ceria units; A-2b - one deposited unit and one in subsurface cavity; A-2c - two units in identical subsurface cavities; A-13b - deposited $\text{Ce}_{12}\text{O}_{24}$ nanoparticle and one CeO_2 unit in subsurface cavity; A-13c - $\text{Ce}_{11}\text{O}_{22}$ deposited, two units CeO_2 in subsurface cavities; B-1b - CeO_2 unit in subsurface cavity; B-1c -one CeO_2 unit in internal cavity; B-2b - two CeO_2 units in identical subsurface cavities; B-4b - three deposited CeO_2 units and one in a subsurface cavity;

Description of the approach for simulation of the relative concentrations of reduced and stoichiometric ceria nanoparticles on γ -Al₂O₃(100) surface using enthalpy and entropy values obtained from computational results.

From the calculated energy values and pertinent vibrational frequencies we determined thermodynamic quantities for different models, which allowed us to analyze the possibilities for creation of O vacancy in the ceria nanoparticles deposited on the alumina surfaces depending on the temperature and oxygen pressure in the system. For this aim we considered the reaction:



We define the relative Gibbs free energy of Ce₁₃O₂₆/Al₂O₃ and Ce₁₃O₂₅/Al₂O₃ systems, $\Delta G(\text{Al}_2\text{O}_3/\text{Ce}_{13}\text{O}_{26-x})$, x = 0 or 1:

$$\Delta G(\text{Al}_2\text{O}_3/\text{Ce}_{13}\text{O}_{26-x}) = \Delta H(\text{Al}_2\text{O}_3/\text{Ce}_{13}\text{O}_{26-x}) - T\Delta S(\text{Al}_2\text{O}_3/\text{Ce}_{13}\text{O}_{26-x}).$$

The enthalpy values, $\Delta H(\text{Al}_2\text{O}_3/\text{Ce}_{13}\text{O}_{26-x})$, were obtained from the total energy values corrected for the internal vibrational energy E_v ¹ and zero-point vibrational energy (ZPE) derived from vibrational frequencies of the oxygen centers, which have been subsequently removed to form reduced structures:

$$H = E_{\text{el}} + E_v + \text{ZPE}.$$

In the calculation of the entropy values of the Al₂O₃/Ce₁₃O_{26-x} structures only the electronic (S_{el}) and vibrational (S_v) degrees of freedom were taken into account, since the O adsorbates are bound to the surface sufficiently strongly and the rotational and translational degrees of freedom are converted into vibrations.^{2,3} Only for the O₂ molecule in the gas phase translational and rotational contributions E_{tr} and E_{rot} are added to the internal energy and entropy:

$$H(\text{O}_2) = E_{\text{el}} + E_v + E_{\text{tr}} + E_{\text{rot}} + \text{ZPE},$$

$$S(\text{O}_2) = S_{\text{el}} + S_v + S_{\text{tr}} + S_{\text{rot}}.$$

The expressions for all enthalpy and entropy contributions can be found elsewhere.¹

-
1. J. W. Ochterski, Thermochemistry in *Gaussian*, 2000, 1-19, www.gaussian.com/g_whitepap/thermo.htm
 2. N. Hansen, T. Kerber, J. Sauer, A. T. Bell and F. J. Keil, *J. Am. Chem. Soc.*, 2010, **132**, 11525-11538.
 3. H. A. Aleksandrov and G. N. Vayssilov, *Catal. Today*, 2010, **152**, 78-87.

Discussion on interatomic distances in the different structures

The number of oxygen centers surrounding the cerium ions and the corresponding average Ce-O distances in the modeled structures are shown Tables 1 to 4. In the structures with deposited one or two CeO₂ units on alumina (100) surface the coordination number of cerium cation is 3 and 4, respectively, with average Ce-O distance, $\langle\text{Ce-O}\rangle$, is in the 203 and 214-219 pm (Table 1). In the structures with incorporated Ce⁴⁺ cations in cavities of alumina, the number of oxygen neighbors, N, increases to 7 or 8, which is accompanied by increase of the average Ce-O distance to 234-252 pm. In most of the structures with two reduced ceria cations, which are incorporated in the bulk of alumina or exchanged with aluminum ions, the number of oxygen neighbors is 7 and $\langle\text{Ce-O}\rangle$ value is 245-250 pm.

The coordination number of the Ce⁴⁺ cations from the nanoparticle on (100) surface, which are incorporated in the cavities or exchanged with Al³⁺ from the bulk of the slab, is 7, while the average Ce-O distance varies between 233 and 238 pm (Table 2). The number of oxygen neighbors of the Ce³⁺ cation incorporated in a cavity is 6 with average $\langle\text{Ce-O}\rangle$ distance of 241 pm.

For the other surface, (001), the coordination number of deposited cerium cations in the structures with one and two units is 5 and the average $\langle\text{Ce-O}\rangle$ distances are around 235 pm (Table 3), both higher than on the (100) surface. The number of oxygen neighbors of cerium cations in cavities is 6 or 8 and the $\langle\text{Ce-O}\rangle$ values are in the range 235-241 pm.

The average distance of the incorporated ceria units from a ceria nanoparticle is 237 pm and the coordination number is six. Similar to the situation on (100) surface, the coordination of exchanged cerium cations in the structures with deposited nanoparticle on (001) surface is 7.